# Analysis of the Thermal Balance Characteristics for Multiple-Connected Piezoelectric Transformers

Joung-Hu Park, *Member, IEEE*, Bo-Hyung Cho, *Senior Member, IEEE*, Sung-Jin Choi, and Sang-Min Lee

***Abstract*—Because the amount of power that a piezoelectric transformer (PT) can handle is limited, multiple connections of PTs are necessary for the power-capacity improvement of PT-applications. In the connection, thermal imbalance between the PTs should be prevented to avoid the thermal runaway of each PT. The thermal balance of the multiple-connected PTs is dominantly affected by the electrothermal characteristics of individual PTs. In this paper, the thermal balance of both parallel-parallel and parallel-series connections are analyzed by electrical model parameters. For quantitative analysis, the thermal-balance effects are estimated by the simulation of the mechanical loss ratio between the PTs. The analysis results show that with PTs of similar characteristics, the parallel-series connection has better thermal balance characteristics due to the reduced mechanical loss of the higher temperature PT. For experimental verification of the analysis, a hardware-prototype test of a $C_s$-$L_p$ type 40 W adapter system with radial-vibration mode PTs has been performed.**

## I. Introduction

Today, the piezoelectric transformer (PT) is widely used in power applications such as isolated power converters and CCFL driving inverters [1], [2]. The PT may become a good alternative solution to the magnetic transformer due to a low profile, no EMI, and no winding area. However, the amount of power that a PT can handle is limited, and if the PT is highly multi-layered for the handling of greater power capacities, then the manufacturing cost increases. To avoid the cost increase and process the power exceeding the single-PT power-handling limit, the use of multiple-connected PTs is indispensable [3]–[6]. For the configuration of multiple PTs, thermal balance is an important issue in avoiding the overheating of the PTs [3]. In previous research, the thermal imbalance problem of the parallel-parallel connection was reported due to the positive temperature coefficient effect of the radial mode disk-type PT [7]. However, further development of the research is required because there also exist some other cases in which the parallel-series connection shows a tendency toward thermal imbalance between other PT samples. To approach the issue, this paper focuses on the loss-determining factors such as the electrical resistance and the resonant impedance (admittance) in the equivalent circuit model. These parameters are supposed to dominate the electrothermal characteristics by affecting either the power-transfer current or the resistance itself [8]. The purpose of this paper is to analyze the relationship between the equivalent circuit parameters and the thermal characteristics, especially regarding the thermal balance issues. The analysis is verified through the hardware experiments using 40 W prototype AC/DC converters.

Manuscript received May 22, 2007; accepted July 28, 2008.

J.-H. Park and B.-H. Cho are with Seoul National University, Department of Electrical Engineering, Seoul, South Korea (e-mail: wait_4_u@hotmail.com).

S.-J. Choi is with PALABS Co., Ltd., Gyeunggi-Do, South Korea.

S.-M. Lee is with Samsung Electronics Co. Ltd., Gyeunggi-Do, South Korea.

Digital Object Identifier 10.1109/TUFFC.2009.1226

## II. Thermal Characteristics of a Single PT

### A. Equivalent Circuit Model of PT

Recently, an application of a radial-mode PT for the powering of a conventional 32 W fluorescent lamp from line power has been reported [9], [10]. These radial mode disk-type piezoelectric transformers were used as the main step-down transformer of the power application in this research; see Fig. 1(a). The primary electrode is located in the center, and the secondary electrodes are concentrically arranged on the outer part of the disk and spaced from the primary electrode. The PT is made of DIT D140 (Dong-Il Technology, Hwasung-Si, Kyonggi-Do, South Korea), a hard ceramic material (PZT-4 series) with the characteristics shown in Table I [11]. The disk is polarized in the axial direction and thus is perpendicular to the plane of the electrodes. This device can be operated in the fundamental radial or the first overtone resonance. The fundamental resonant frequency is around 60 kHz, and the secondary resonant frequency is about 150 kHz [8]. Fig. 1(b) shows the equivalent circuit model of the PT, and a detailed analysis is performed using these model parameters. In the model, $R_m$ represents the mechanical loss factors such as friction, and $i_m$ is the current flowing through it. Because $R_m$ is the single source of the power loss ($P_m = {i_m}^2 R_m$) in the model, $R_m$ is supposed to drive the PT temperature by dissipating heat. Therefore, $P_m$ is the most critical factor when determining the thermal characteristics and can be used as a determinant parameter for the thermal balance analysis of multiple PTs.

### B. Equivalent Inductance to Resonant Tank of PT

In the equivalent circuit model, there are 3 parameters ($R_m$, $L_m$, $C_m$) that determine the resonant impedance

TABLE I. PARAMETER VALUES OF LOW-TEMPERATURE-FIRING MATERIAL, DIT D140 [8].

| Item | Characteristics |
|---|---|
| Coupling Coefficient, $k_p$ | 0.60 |
| Dielectric Loss, tan $\delta$ | 0.003 |
| Relative Dielectric Constant, $\varepsilon_{33}^{T}/\varepsilon_0$ | 1500 |
| Piezoelectric Constant, $d_{33}$ | $380 \times 10^{-12}$ C/N |
| Quality Factor, $Q_m$ | 800 |
| Temperature Coefficients of Capacitance, 25–100°C | 3000 ppm/°C |

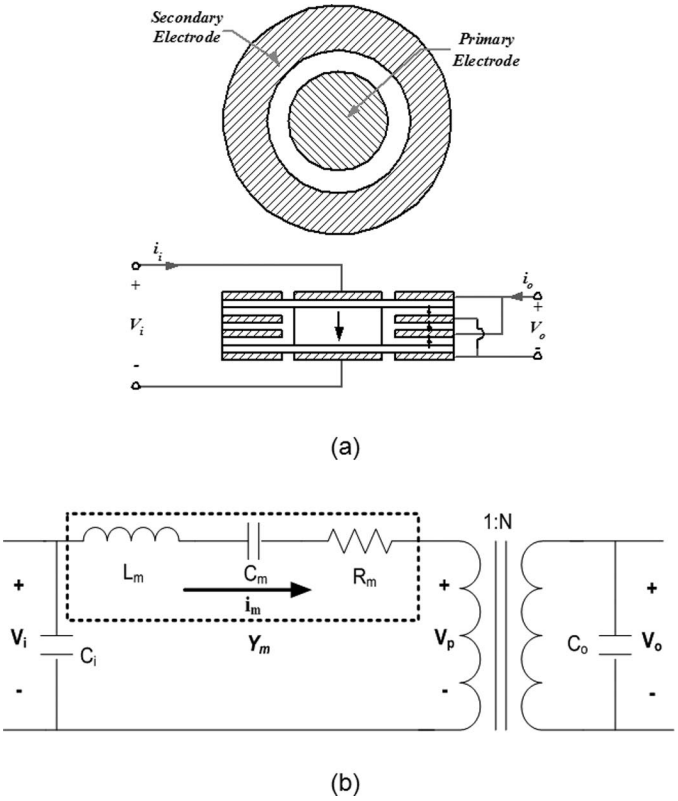


Fig. 1. Physical configuration (a) and equivalent circuit model (b) for the piezoelectric transformer [8].

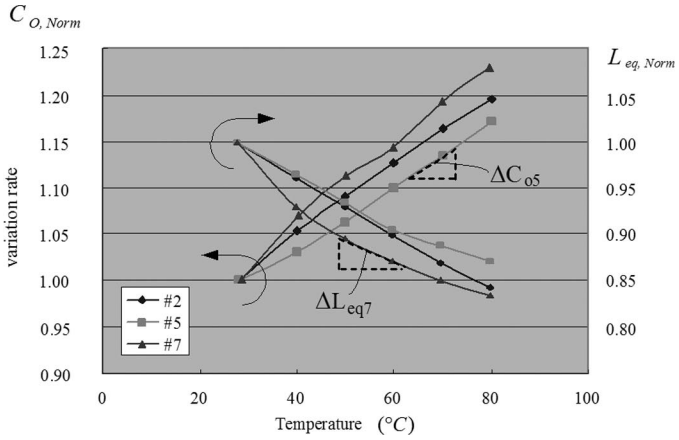


Fig. 2. Resonant frequency and characteristic impedance parameter variation of 2 PTs (index #2, #5, #7) according to temperature rise.

in the mechanical resonance branch. Thus, when an $n$ amount of multiple PTs are analyzed, the total number of the variables increases to $3n$, which complicates the analysis procedures and makes analysis very difficult. Therefore, it is necessary to represent the resonant branch with equivalent single impedance simplified for design-oriented analysis.

The simplifying procedure is as follows. First, we assume that the operating range is very close to the resonant frequency. In the range, because the series resonant Q-factor ($= Z_c / R_m$, where $Z_c$ is characteristic impedance) is very high (>200) due to the negligible $R_m$, the resonant parameters $L_m$ and $C_m$ are replaced with both $Z_c$ and the resonant frequency ($\omega_r$) for representing more simplified equations. In this paper, the operating frequency is set to 150 kHz not only for the PT's resonant frequency but also for the maximum efficiency operation with the heaviest load—the condition that is most critical to the thermal balance problem. Because the operating frequency range is located slightly higher than the resonant frequency by several kilohertz, the resonant branch impedance has approximately a 90° phase shift, which has an effect similar to an inductor. Therefore, the resonant branch can be represented as an equivalent inductance:

$$L_{\text{eq}} = Z_c \left( \frac{1}{\omega_r} - \frac{\omega_r}{\omega_s{}^2} \right) \tag{1}$$

where $\omega_s$ is the input voltage frequency.

The simplification is reasonable because the resonant impedance keeps almost the same 90° phase shift (inductive) just with the inductance change in the maximum-gain frequency range. Therefore, determining the intuitive derivation without significant errors is possible due to the simplified parameter.

### C. Thermal Variation of PT Parameters

The equivalent parameters in previous sections vary according to the temperature change of the single piezoelectric transformer. For example, as the temperature rises, the characteristic impedance of a group of radial mode PTs proportionally decreases at the above-resonant operating frequency. Because $L_{\text{eq}}$ is proportional to the impedance, $L_{eq}$ decreases with the temperature rise as well (see Fig. 2).

The analyzing parameters describing thermal behavior are defined as the electrothermal parameters. The parameters are the relative values normalized by the parameters

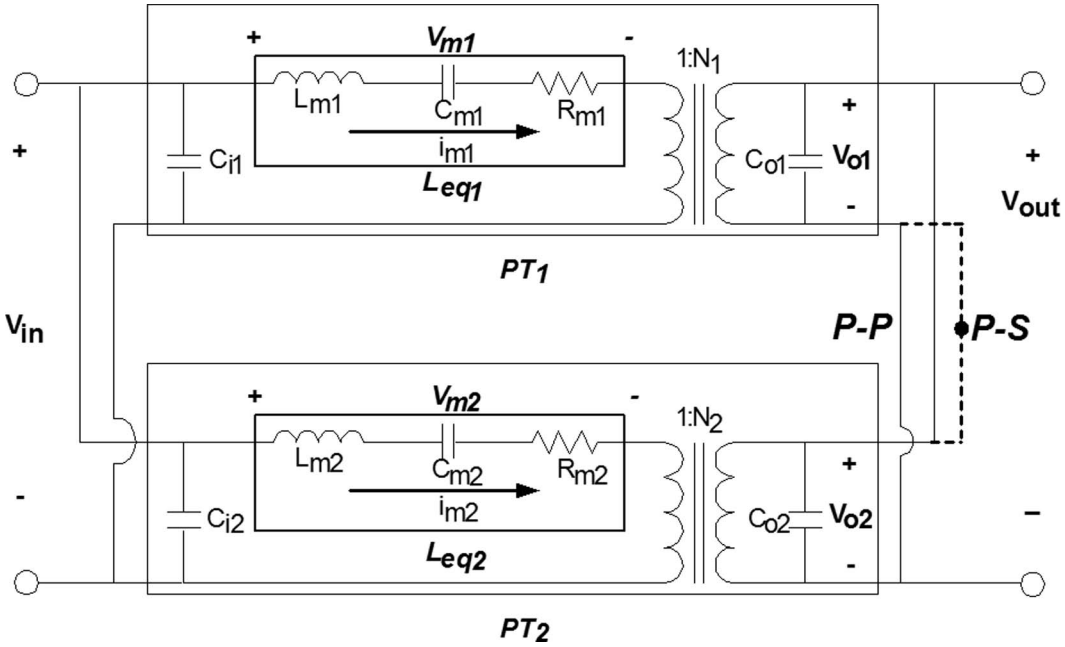


Fig. 3. Multiple connections of PTs (parallel-parallel (P-P) connection and parallel-series (P-S) connection) [5].

at room temperature. The change rates of the PTs according to temperature, such as the input and the output capacitances, $L_{\text{eq}}$, and mechanical resistance are denoted as $\Delta C_i$, $\Delta C_o$, $\Delta L_{\text{eq}}$, and $\Delta R_m$, respectively (see Fig. 2). Fig. 2 shows some measured data examples of the electrothermal parameters such as normalized $C_o$ ($C_{o,\text{norm}}$) and normalized $L_{\text{eq}}$ ($L_{\text{eq,norm}}$) according to thermal change from 30 to 80°C. Slope of each measured curves means $\Delta C_o$ and $\Delta L_{\text{eq}}$. The transformer turn ratio, $N$, is out of consideration because of its thermally invariant characteristics. Due to the fact that both $\omega_s$ and $\omega_r$ are almost constant against thermal variations, the resonant impedance $\Delta Z_c$ can be replaced into $\Delta L_{\text{eq}}$ in Fig. 2; see (1). Using the thermal-variant parameter of $\Delta L_{\text{eq}}$, multiple-PT thermal balance problems are approached.

## III. Thermal-Balance Analysis of Multiple PTs

Thermal variations of the single PT parameters affect the thermal balance among multiple PTs. In the equivalent circuit model, the mechanical loss on the damping resistance $R_m$ is the dominant factor determining the PT temperature. Therefore, the thermal behavior of multiple PTs can be estimated by examining the loss factor of each PT. For example, when high-temperature PT has a smaller power loss than the other low-temperature PT, temperature imbalance can be relieved. This is a kind of thermally negative feedback operation because when a temperature-difference disturbance ($\Delta T$) occurs between a pair of PTs, the disturbance is automatically suppressed by feedback action of the decreased loss-dissipation factor ($\Delta P$) caused by $\Delta T$. On the contrary, if the high-temperature PT moves into relatively higher power loss with the temperature rise, then the positive feedback of the thermal operation causes the imbalance between the PTs. To develop the quantitative analysis of the feedback action, a performance index parameter, called relative-loss $\Delta P_m$ ($= P_{m2}/P_{m1}$), is introduced. $P_{m1}$ is power loss of the reference PT, and $P_{m2}$ is the loss of the other PT. When $\Delta P_m$ is calculated at each bias condition such as temperature ($T$) and $\Delta T$, the thermal balance dynamics of the 2 PTs can be predicted. From the analysis, the structure that is more feasible for thermal balance in multi-connected PTs, either parallel-parallel or parallel-series, can be found. In Section III-A, the analysis will be performed with the electrothermal parameters of the PT example presented in Fig. 2, and in Section III-B, circuit parameter deviations will be included in the analysis.

### *A. Derivation of the Loss Factors*

Fig. 3 (solid line connection in the PT's output port) shows the parallel-parallel (P-P) connection of the 2 PTs [7]. The voltage across the resonant branch is determined by the same input and output voltages. Thus, the resonant currents ($i_{m1}$, $i_{m2}$) can differ from each other only due to the variation of $L_{\text{eq}}$ and $R_m$ [7]:

$$\begin{aligned} P_{m1} : P_{m2} &= i_{m1}^2 R_{m1} : i_{m2}^2 R_{m2} \\ &= R_{m1}\frac{1}{{L_{\text{eq1}}}^2} : R_{m2}\frac{1}{{L_{\text{eq2}}}^2} = R_{m1}{L_{\text{eq2}}}^2 : R_{m2}{L_{\text{eq1}}}^2 \\ \text{where } R_{m2} &= R_{m1}(1+\Delta R_m \Delta T), \\ L_{\text{eq2}} &= L_{\text{eq1}}(1+\Delta L_{eq}\Delta T). \end{aligned} \tag{2}$$

Thus, the relative power loss rate in P-P is described as

$$\Delta P_m = \frac{P_{m2}}{P_{m1}} = \frac{1+\Delta R_m \Delta T}{(1+\Delta L_{\text{eq}}\Delta T)^2}. \tag{3}$$

$$
\begin{aligned}
P_{m1} : P_{m2} &= R_{m1}\left\{\left(\frac{C_{o1}}{\omega_s L_{\mathrm{eq1}} L_{\mathrm{eq2}} N^2} - \frac{\omega_s C_{o1} C_{o2}}{L_{\mathrm{eq1}}}\right)^2 + \left(\frac{2}{\omega_s^2 L_{\mathrm{eq1}} L_{\mathrm{eq2}} R_{\mathrm{eq}} N^2} - \frac{C_{o1}+C_{o2}}{L_{\mathrm{eq1}} R_{\mathrm{eq}}}\right)^2\right\} \\
&: R_{m2}\left\{\left(\frac{C_{o2}}{\omega_s L_{\mathrm{eq1}} L_{\mathrm{eq2}} N^2} - \frac{\omega_s C_{o1} C_{o2}}{L_{\mathrm{eq2}}}\right)^2 + \left(\frac{2}{\omega_s^2 L_{\mathrm{eq1}} L_{\mathrm{eq2}} R_{\mathrm{eq}} N^2} - \frac{C_{o1}+C_{o2}}{L_{\mathrm{eq2}} R_{\mathrm{eq}}}\right)^2\right\} \\
&\cong 1 : (1+\Delta R_m \Delta T)(1+\gamma) \cong 1 : 1 + \Delta R_m \Delta T + \gamma \quad \text{where} \\
R_{m2} &= R_{m1}(1+\Delta R_m),\ L_{\mathrm{eq2}} = L_{\mathrm{eq1}}(1+\Delta L_{\mathrm{eq}}),\ C_{o2} = C_{o1}(1+\Delta C_o), \\
A &= \frac{C_{o1}}{\omega_s L_{\mathrm{eq1}} L_{\mathrm{eq2}} N^2} - \frac{\omega_s C_{o1} C_{o2}}{L_{\mathrm{eq1}}}, \\
B &= \frac{2}{\omega_s^2 L_{\mathrm{eq1}} L_{\mathrm{eq2}} R_{\mathrm{eq}} N^2} - \frac{C_{o1}+C_{o2}}{L_{\mathrm{eq1}} R_{\mathrm{eq}}}, \\
\alpha &= \frac{C_{o1}\Delta C_o \Delta T}{\omega_s L_{\mathrm{eq1}} L_{\mathrm{eq2}} N^2} + \frac{\omega_s C_{o1} C_{o2}}{L_{\mathrm{eq1}}}\Delta L_{\mathrm{eq}} \Delta T, \\
\beta &= \frac{C_{o1}+C_{o2}}{L_{\mathrm{eq1}} R_{\mathrm{eq}}}\Delta L_{\mathrm{eq}} \Delta T, \\
\gamma &= \frac{2A\alpha + 2B\beta}{A^2 + B^2}.
\end{aligned}
\tag{4}
$$

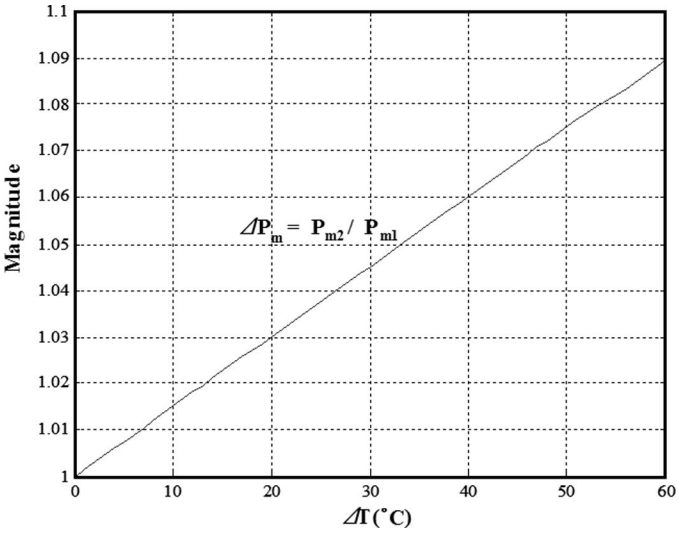


Fig. 4. Relative loss curve of the radial-mode PTs in P-P structure.

Fig. 4 shows the relationship between the temperature difference and the loss factor. As shown in the figure, $\Delta P_m$ is always greater than unity and the factor increases as $\Delta T$ increases. Therefore, it is supposed that higher temperature $PT_2$ has higher loss, and the temperature difference will be greater as the operating time increases. The analysis shows that even though there is no equivalent-circuit and electrothermal parameter differences between the PTs, the thermal balance in P-P structure would be hard to maintain due to the thermally positive feedback responses.

Fig. 3 (dotted-line connection in the PT's output port) shows the configuration of the parallel-series (P-S) connection, as well. As in the analysis of the P-P case, the electrothermal parameters are assumed identical. However, the voltages across the resonant branches ($L_{\mathrm{eq1}}$, $L_{\mathrm{eq2}}$ in Fig. 3) are different from each other due to the difference of the output voltages, unlike the P-P case. In the P-S configuration, $\Delta P_m$ is derived as (4) (see above).

$R_{\mathrm{eq}}$ is the equivalent load resistance. Using these equations, the loss factor $\Delta P_m$ can be derived. The final equation is complicated and is simplified with 2 variables $\Delta R_m$ and $\gamma$, which are the $\Delta L_{\mathrm{eq}}$ and $\Delta C_o$ effects on the resonant current. Based on these equations, the loss parameter $\Delta P_m$ can be derived.

Fig. 5 shows the relationship between the temperature difference and the loss factor in the P-S configuration. As shown in the figure, $\Delta P_m$ is always less than unity, and the factor decreases as $\Delta T$ increases. Therefore, it is supposed that higher temperature $PT_2$ has lower loss, and the temperature difference will be smaller. The analysis shows that if there is no parameter difference between the PTs, the P-S structure will have thermal balance due to the thermally negative feedback responses.

### *B. Consideration of the Circuit Parameter Deviation among PTs*

Circuit parameter deviations among PTs as well as the electrothermal parameters affect the thermal balance of multiple PTs. In this section, the effects are analyzed both in P-P and P-S configurations.

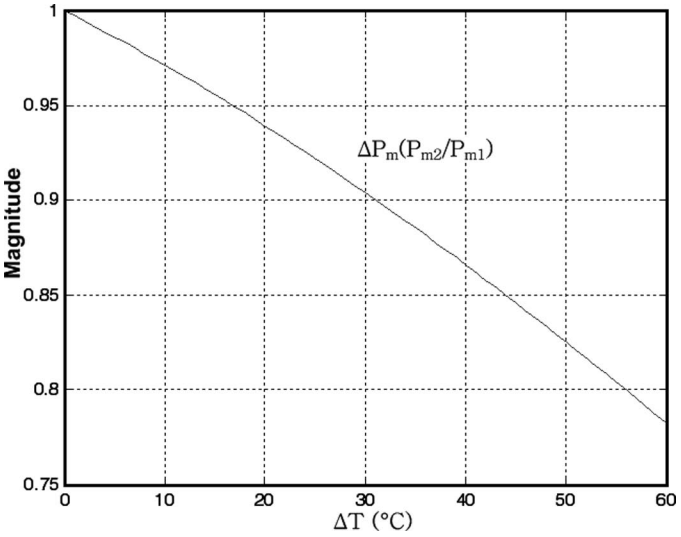


Fig. 5. Relative loss curve of the radial-mode PTs in P-S structure.

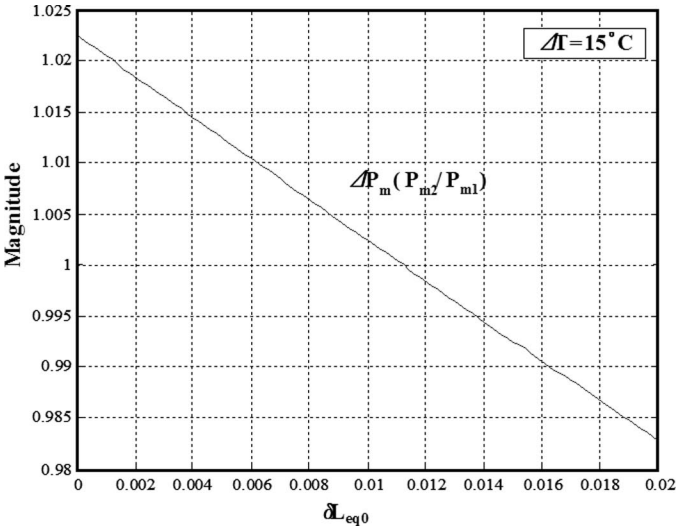


Fig. 6. The loss factor of P-P configuration according to $\delta L_{\mathrm{eq0}}$.

*1) P-P Configuration:* As shown in (2), $L_{\mathrm{eq}}$ affects the thermal balances in P-P configurations. Therefore, it is supposed that the parameter difference of $L_{\mathrm{eq}}$ would significantly change the thermal balance with given $\Delta L_{\mathrm{eq}}$. The analysis conditions are as follows:

$$\begin{aligned} &\text{Temperature difference: } T_{\mathrm{PT2}} = T_{\mathrm{PT1}} + 15^{\circ}\mathrm{C}. \\ &\text{Then, } L_{\mathrm{eq2}} = L_{\mathrm{eq1}}(1 + \delta L_{\mathrm{eq0}})(1 + 15 \cdot \Delta L_{\mathrm{eq}}) \end{aligned} \tag{5}$$

where the inductance difference rate is $\delta L_{\mathrm{eq0}} = \mathrm{L_{eq2}}/\mathrm{L_{eq1}} - 1$ (no unit) at the bias temperature $T$.

Substituting (5) into (2), the relationship between $\Delta P_m$ and $\delta L_{\mathrm{eq0}}$ is derived as shown in Fig. 6. In the figure, it is shown that the greater $\delta L_{\mathrm{eq0}}$ is, the more $\Delta P_m$ decreases. Therefore, it is more profitable to thermal balance in P-P structure that a PT pair has a high inductance parameter difference from each other.

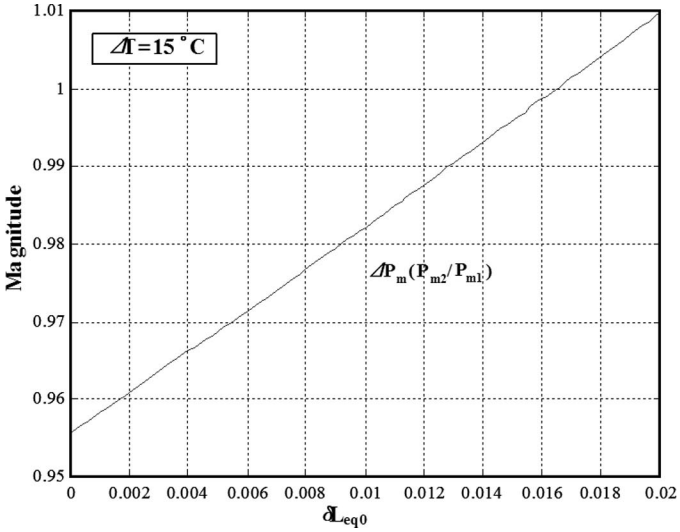


Fig. 7. The loss factor of P-S configuration according to $\delta L_{\mathrm{eq0}}$.

*2) P-S Configuration:* Thermal balance characteristics of radial-mode PTs in P-S structure are examined based on the deviation rates of $L_{\mathrm{eq}}$ and $C_o$ ($\delta C_{o0}$, no unit); see (6). The analysis conditions are as follows:

$$\begin{aligned} &\text{Temperature difference: } T_{\mathrm{PT2}} = T_{\mathrm{PT1}} + 15^{\circ}\mathrm{C}. \\ &\text{Then, } L_{\mathrm{eq2}} = L_{\mathrm{eq1}}(1 + \delta L_{\mathrm{eq0}})(1 + 15\Delta L_{\mathrm{eq}}) \\ &\text{and } C_{o2} = C_{o1}(1 + \delta C_{o0})(1 + 15\Delta C_o) \end{aligned} \tag{6}$$

where the capacitance difference rate is $\delta C_{o0} = C_{o2}/C_{o1} - 1$ (no unit) at the bias temperature.

Substituting (6) into (4), the relationship between $\Delta P_m$ and $\delta L_{\mathrm{eq0}}$ is derived as shown in Fig. 7. From the figure, the greater $\delta L_{\mathrm{eq0}}$ is, the greater $\Delta P_m$ becomes. Therefore, it is undesirable to the thermal balance that a PT pair has a high inductance deviation.

In the same manner, the relationship between $\Delta P_m$ and $\delta C_{o0}$ is derived as shown in Fig. 8. From the figure, the greater $\delta C_{o0}$ is, the greater $\Delta P_m$ becomes. In other words, it is undesirable to thermal balance that a PT pair has a high output capacitance difference between the PTs.

From the analysis, it can be seen that in P-P configuration, circuit parameter deviations among PTs positively contribute to the thermal balance. On the other hand, P-S configuration requires high uniformity among the PT parameters in multiple connection. Therefore, when we design a high-power application with multiple-connected PTs from any radial-mode PT set in excellent equivalent-circuit and electrothermal parameter uniformity, P-S connection is recommended for thermal balance.

## IV. Operation Example of Small Circuit-Parameter Deviation

In this section, the proposed thermal balance analysis is verified by hardware experiments of real PTs by estimating the loss factor at every bias point.

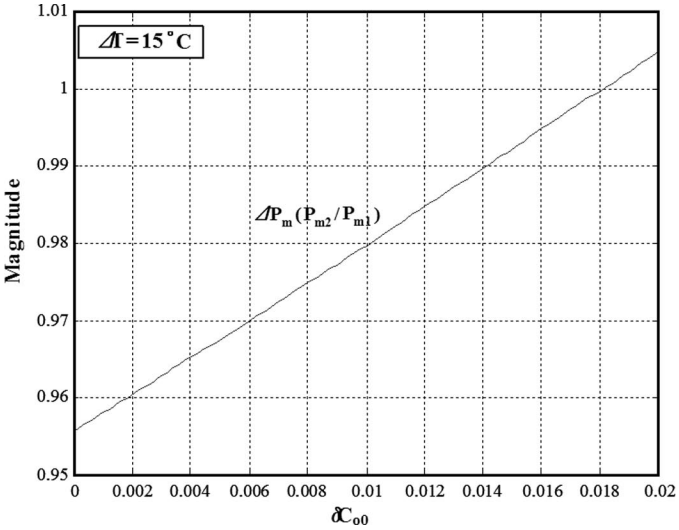


Fig. 8. The loss factor of P-S configuration according to $\delta C_{o0}$.

TABLE II. Circuit Parameters of Real PT Samples.

| | PT #2 | PT #5 | PT #7 |
|---|---|---|---|
| $L_{eq}$ | 847 uH | 891 uH | 696 uH |
| $C_o$ | 18.9 nF | 19.2 nF | 18.7 nF |
| $N$ | 0.2 | 0.2 | 0.2 |

Consider an example of radial-vibration mode PT samples with circuit parameters in Table II (measured by network analyzer HP4194; Hewlett Packard, Palo Alto, CA) and with electrothermal ones in Fig. 2. As shown in Table II, PT samples #2 and #5 have very small parameter deviations similar to the case described in Section III-A. On the other hand, samples #2 and #7 have significant parameter deviations like the one described in Section III-B. From the analysis results in Section III, the #2 and #5 pair should have thermal balance in P-S structure, and the #2 and #7 pair in P-P structure. In this section, a small deviation example will be presented and analyzed with the real PT parameters, and a large deviation case will be examined in Section V. The analysis will be verified from the hardware experiment also.

### *A. Numerical Analysis with Various PT Temperature Biases*

In the previous section, the influences of electrothermal characteristics and circuit parameter deviations were considered according to $\Delta T$ bias condition. In this section, using Matlab (MathWorks, Natick, MA), thermal behaviors on every operating temperature bias points are predicted. With measured data given in Fig. 2 and Table II, the loss factor can be calculated. Fig. 9 shows the loss-factor simulation results of PT#2 and #5 combination in both P-P and P-S connections. The x axis is the PT bias temperature and the y axis is the loss factor, which represents relative power dissipation on each PT. Each line in the plot represents the operating points of the same bias $\Delta T$. The solid line at Magnitude = 1 is the PT

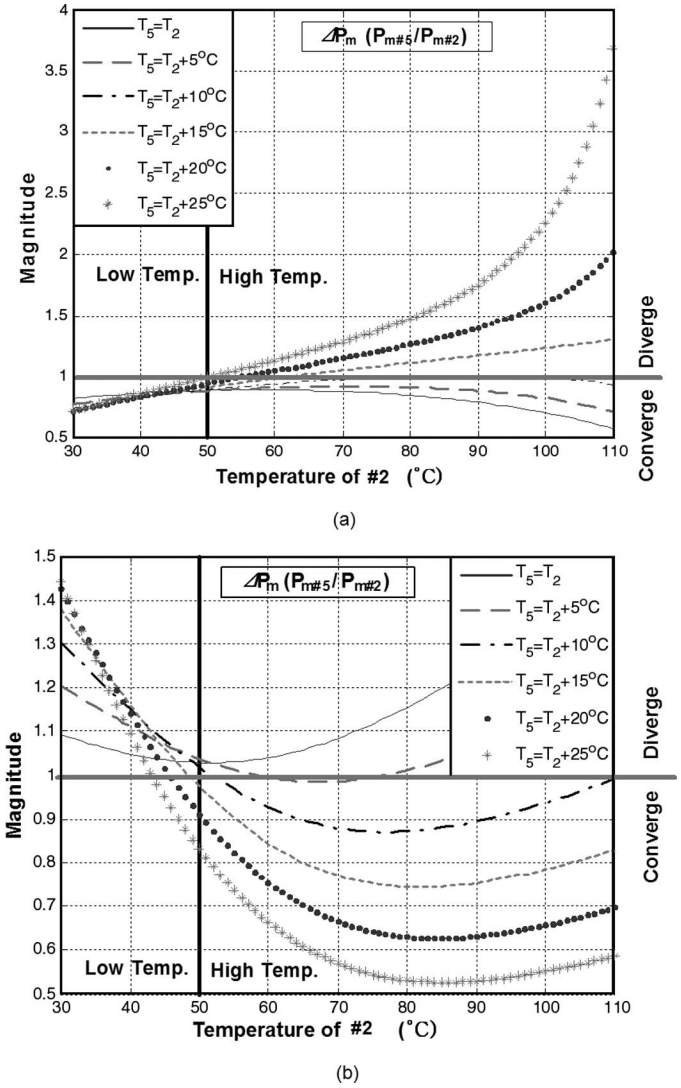


Fig. 9. Loss ratio curves of (a) parallel-parallel and (b) parallel-series of PT #2 and #5.

pair's thermal dynamic criterion between the temperature convergence (negative feedback) and divergence (positive feedback) area. From this simulation curve, it can be estimated how the PT pair performs in thermal balance at every operating bias point. The PT temperature region is also divided into 2 parts, such as low-temperature and high-temperature regions for convenient descriptions below. The boundary is 50°C, because around the temperature, most of the loss curves change the thermal behavior by crossing the criterion, then the analysis is possible even with decoupling of bias $\Delta T$ effects. Generally, PT temperature moves from a low-temperature region into a high-temperature region by thermal excitement. With the criterion and the boundary, there can be 4 cases: (1) low temperature region–converge; (2) low temperature region–diverge; (3) high-temperature region—converge; and (4) low-temperature region–diverge.

From the P-P curves in Fig. 9(a), it can be seen that the #2 and #5 pair has excellent thermal balance characteristics due to the converging performance in the low-temperature region whatever the bias $\Delta T$ is. However, in

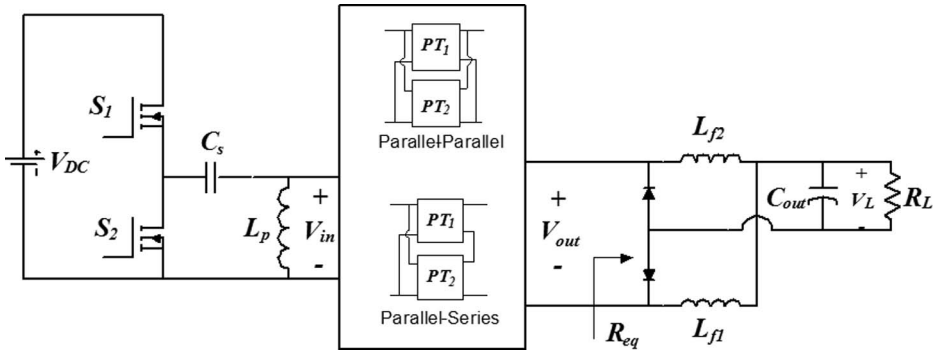


Fig. 10. *Cs-Lp* type adapter using multiple connection of PT [5].

the high-temperature region, the overall thermal balance characteristics become worse due to the change of the loss factor into diverging criteria at every bias condition except very small $\Delta T$. From this analysis, it is supposed that during the front period of excitement process, the PT pair would have small temperature differences; however, the temperatures diverge as they are approaching full excitement. In the same manner, the thermodynamic simulation of the P-S configuration can be estimated. Fig. 9(b) shows that the pair has poor thermal balance characteristics in the low-temperature region because most of the operation curves are located in divergence region whatever the bias $\Delta T$ is. However, as the PTs warm up into the high-temperature region, the overall thermal balance characteristics are recovered due to the change of the loss factor into diverging criteria at every bias condition except low bias condition $\Delta T < 10$°C. From this analysis, it is supposed that the thermodynamic behavior would be totally opposite from P-P case such that during the initial period of the excitement process, the PT pair would have high-temperature differences; however, the temperatures converge as they are approaching full excitement. This thermally negative-feedback operation contributes to the temperature balance between the multiple PTs. However, there will still exist a temperature gap at full excitement around 10 to 20°C because some bias condition $\Delta T < 10$°C still maintains its $\Delta P$ over unity. In following section, this analysis will be verified by the hardware experiment.

### *B. Hardware Verification*

The multiple-connections of the 20 W power-capacity PTs are used in a 40 W adapter prototype, which employs a $C_s$-$L_p$ type resonant half-bridge topology as shown in Fig. 10 [12]. A current doubler is employed as the output rectifier, and the equivalent load, $R_{\rm eq}$, is $\pi^2 R_L/2$. To operate each PT at the optimal load $R_{\rm eq}$, the load resistances of the adapter in the parallel-parallel connection and the parallel-series connection are $R_{\rm eq}/2$ and $2R_{\rm eq}$, respectively. The circuit component and PT parameter values are shown in Tables I and II.

The hardware prototype used for the multiple-connection PT test is as follows:

- Optimal load of the single PT ($R_{\rm eq}$): 50 Ω
- Operating frequency ($\omega_s$): 150 kHz (maximum gain frequency)
- *Cs/Lp*: 30 nF/0.3 mH
- $V_{\rm DC}/V_L$ (power/$R_L$) in parallel-parallel connection: 210 V/14 V (39.2 W/5 Ω)
- $V_{\rm DC}/V_L$ (power/$R_L$) in parallel-series connection: 210 V/28 V (39.2 W/20 Ω)

Fig. 11(a) and (b) shows the temperature trajectories of the PTs in the P-P and P-S connections, respectively. The temperature measurements of the PT were performed by a thermo-coupler and were recorded by a Mobile Corder MV200 (Yokogawa, Tokyo, Japan). The measurement spot is the primary electrode, the hottest part [13]. The figures show that in the low-temperature region, the P-P connection has a superior balance performance compared to the P-S connection. However, crossing into the high-temperature region, the P-P connection has an unbalanced dynamic and diverges up to about a 34.4°C temperature difference. On the contrary, the P-S configuration maintains the thermal balance by just 17.7°C $\Delta T$. This result agrees well with the thermal balance prediction of the analysis in the previous section.

## V. Operation Example of Large Circuit-Parameter Deviation

In this section, another practical case with large circuit parameter deviations as presented in Section III-B will be investigated. With measured data of the PT #2 and #7, the loss factor can be calculated in the same manner as described in Section IV. Fig. 12 shows the simulation and hardware test results of P-P connected PT #2 and #7 in large circuit parameter deviations. From these simulation curves in Fig. 12(a), it can be estimated how the PT pair performs in thermal balance at every bias operating point. Because the PTs have almost the same electrothermal parameters shown in Fig. 2, the overall configuration patterns of the curves are quite similar to those of the PT #2 and #5 P-P connection—see Fig. 9(a)—except for a shift toward the x axis by around 20°C positive caused by

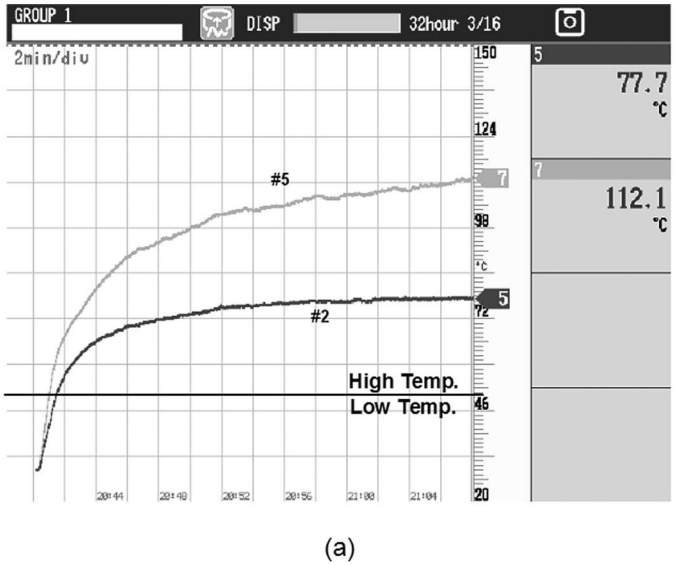


Fig. 11. Hardware test results of (a) parallel-parallel and (b) parallel-series of PT#2 and #5.

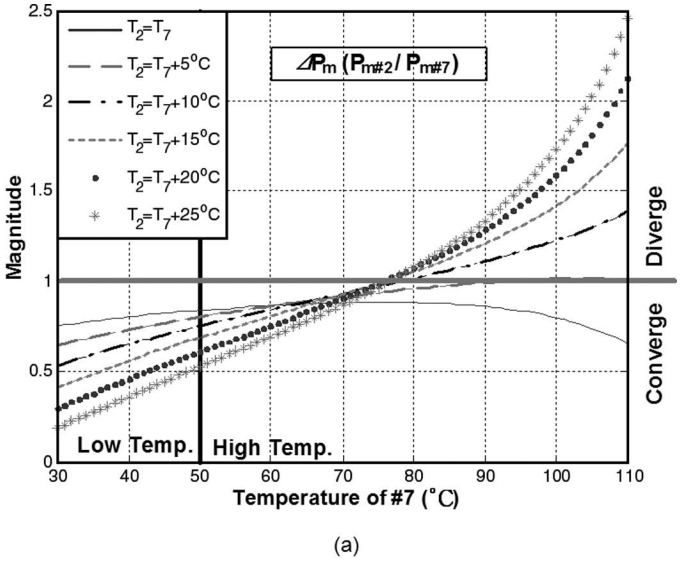


Fig. 12. Simulation (a) and test results (b) of parallel-parallel connected PT #2 and #7 in large equivalent circuit parameter deviations.

the equivalent-circuit parameter deviations. Therefore, it is shown that the parameter deviations contribute to the thermal balance of radial mode PZT PTs in P-P as shown in Section III-B. The hardware verification is shown in Fig. 12(b). PT #2 and #7 temperatures are well balanced both in low-temperature and high-temperature regions, and final $\Delta T$ is just 6°C. Therefore, the prediction by the numerical analysis agrees well with the hardware experiment showing that the high-temperature characteristics are improved by parameter deviation, compared with the result of PT#2 and #5 in Fig. 11(a). From the result, it is shown that P-P connection with given PT devices are the optimal configurations for thermal balance. However, there exists some possibility of the balance breakdown according to Fig. 12(a) if the temperature equilibrium (steady-state) occurs over 90°C due to external disturbances or other causes.

The parallel-series case is also considered in Fig. 13. From this simulation curve in Fig. 13(a), it can be estimated how the PT pair performs in thermal balance at every bias operating point. As with the P-P case, the overall configuration patterns of the P-S curves are also quite similar to the patterns of PT #2 and #5 P-S—see Fig. 9(b)—except for a shift toward the x axis by around 20°C positive caused by the equivalent-circuit parameter deviations. Therefore, unlike the P-P case, the parameter deviations deteriorate the thermal balance of radial mode PZT PTs in P-S exactly as shown in Section III-B. The hardware verification is shown in Fig. 13(b). PT #2 and #7 temperatures are rapidly unbalanced even in the low-temperature region, and the temperature gap increases in the high-temperature region also, with 24°C final $\Delta T$. Therefore, the prediction by the numerical analysis agrees well with the hardware experiment showing that the high-temperature characteristics are deteriorated by parameter deviation, compared with the result of PT#2 and #5 in Fig. 11(b). From the result, it is shown that the P-P connection is more suitable to radial-mode PTs with high parameter deviation for the thermal balance performance.

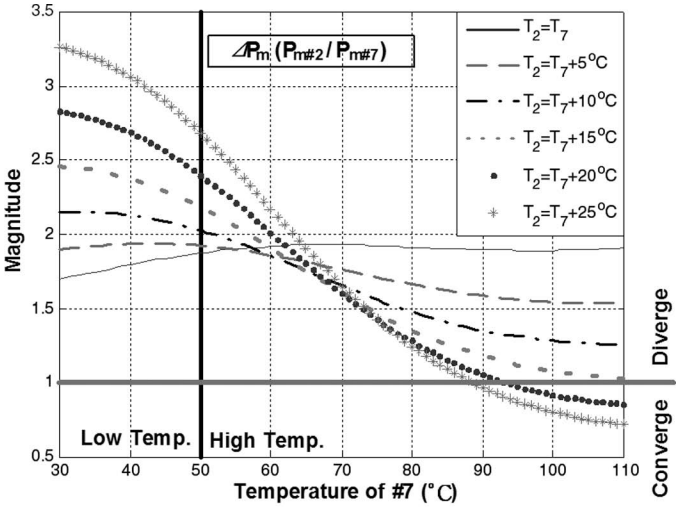


Fig. 13. Simulation (a) and test results (b) of parallel-series connected PT #2 and #7 in large equivalent circuit parameter deviations.

## VI. Conclusions

The thermal balance issues for the multiple connection of the radial-mode disk-type PT have been investigated. The key parameters related to the electrothermal characteristics are extracted from the electrical circuit model, and the relationships among them are derived in the case of both parallel-parallel and parallel-series connections. The thermal balance analysis has been verified through the experimental results using a 40 W resonant half-bridge AC/DC converter. From the results, it is shown that parallel-series connection is more suitable to the multiple-connected radial-mode PZT PTs for thermal balance. However, if the PTs have high parameter deviations, then parallel-parallel connection is more suitable. Future work is to investigate thermal balance features of different type PTs and to make the loss-factor analysis more refined by including dielectric loss and other loss factors.

## References

[1] H. Shin, H. Ahn, and D. Han, "Design analysis of step-down multilayer piezoelectric transformer," *J. Power Electron.*, vol. 3, no. 2, pp. 139–144, Apr. 2003.

[2] G. Chung and K. D. T. Ngo, "Analysis of an AC/DC resonant pulse power converter for energy harvesting using a micro piezoelectric device," *J. Power Electron.*, vol. 5, no. 4, pp. 247–256, Oct. 2005.

[3] S. Bronstein, G. Ivensky, and S. Ben-Yaakov, "Parallel connection of piezoelectric transformers," in *IEEE Power Electronics Specialists Conf. Record*, Jun. 2004, pp. 1779–1785.

[4] S. W. Fung and M. H. Pong, "An improved piezoelectric transformer model with parallel connection feature," in *IEEE Power Electronics Systems and Applications Record*, Nov. 2004, pp. 210–215.

[5] Y. Li and W. Chen, "AC-DC converter with worldwide range input voltage by series and parallel piezoelectric transformer connection," in *IEEE Power Electronics Specialists Conf. Record*, Jun. 2004, pp. 2668–2671.

[6] K. F. Kwok, P. Dong, K. W. E. Cheng, K. W. Kwok, Y. L. Ho, and X. X. Wang, H.Chan, "General study on piezoelectric transformer," in *IEEE Power Electronics Systems and Applications Record*, Nov. 2004, pp. 216–220.

[7] S. Lee, S. Choi, S. Yun, Bo H. Cho, "Input parallel-output series connection of radial mode disk-type piezoelectric transformer for thermal balance improvement," in *IEEE Power Electronics Specialists Conf. Record*, Jun. 2006, pp. 2994–2998.

[8] S. Choi, "Modeling and analysis of disk-type piezoelectric transformer and its application of off-line power converters," Ph.D. dissertation, Seoul National Univ., Seoul, Korea, Feb. 2006.

[9] J. Zhou, F. Tao, and C. F. Lee, "Inductor-less charge pump PFC electronic," in *Proc. 2001 IEEE Industry Application Conf.*, Oct. 2001, pp. 524–529.

[10] R.-L. Lin, F. C. Lee, E. M. Baker, and D. Y. Chen, "Inductor-less piezoelectric ballast for linear fluorescent lamp," in *IEEE Applied Power Electronics Conf. 2001*, Mar. 2001, pp. 664–669.

[11] J.-H. Park, S.-M. Lee, S.-J. Choi, and B.-H. Cho, "Design consideration of parallel–parallel connected piezoelectric transformer for thermal balances," *Jpn. J. Appl. Phys.*, vol. 46, no. 10B, pp. 7067–7072, Oct. 2007.

[12] S. J. Choi, T. I. Kim, S. M. Lee, and B. H. Cho, "Modeling and characterization of radial-mode disk-type piezoelectric transformer for AC/DC adapter," *IEEE Power Electronics Specialists Conf. Record*, Jun. 2005, pp. 624–629.

[13] H. Joo, C. Lee, J. Rho, and H.-K. Jung, "Analysis of temperature rise for piezoelectric transformer using finite-element method," *IEEE Trans. Ultrason. Ferroelectr. Freq. Control*, vol. 53, pp. 1449–1457, Aug. 2006.

**Joung-Hu Park** (M'07) was born in Korea in 1975. He received his B.S, M.S., and Ph.D. degrees from the Electrical Engineering and Computer Science Department of Seoul National University, Seoul, South Korea, in 1999, 2001, and 2006, respectively. He is currently a postdoctoral researcher at Seoul National University. His interests include analysis and design of high-frequency switching converters, renewable energy systems, and piezoelectric transformer power applications.

**Bo-Hyung Cho** (M'89–SM'95) was born in Korea in 1952. He received the B.S. and M.E. degrees in electrical engineering from California Institute of Technology, Pasadena, and the Ph.D. degree, also in electrical engineering, from Virginia Polytechnic Institute and State University (Virginia Tech), Blacksburg. Prior to his research at Virginia Tech, he worked for two years as a member of the technical staff of the Power Conversion Electronics Department, TRW Defense and Space System Group, where he was involved in the design and analysis of spacecraft power processing equipment. From 1982 to 1995, he was a professor in the Department of Electrical Engineering, Virginia Tech. He joined the School of Electrical Engineering, Seoul National University, Seoul, Korea, in 1995, and he is presently a professor. He also is the chairman of the Korean Institute of Power Electronics (KIPE). His main research interests include power electronics, modeling, analysis and control of spacecraft power processing equipment, power systems for space station and space platform, and distributed power

systems. Dr. Cho was a recipient of the 1989 Presidential Young Investigator Award from the National Science Foundation. He is a member of Tau Beta Pi.

**Sung-Jin Choi** (S'05–M'06) was born in Korea in 1973. He received B.S., M.S., and Ph.D. degrees from the Electrical Engineering and Computer Science Department of Seoul National University, Seoul, Korea, in 1996, 1998, and 2006, respectively. He is currently the CTO of PALABS Co., Ltd., Gyeunggi-Do, South Korea, developing power supplies for laptop computers with piezoelectric components. His research interests are in the analysis and design of high-frequency switching converters and portable power supplies using piezoelectric transformers.

**Sang-Min Lee** was born in Korea in 1981. He received his B.S., and M.S. degrees from the Electrical Engineering and Computer Science Department of Seoul National University, Seoul, Korea, in 1999 and 2001, respectively. He is currently an assistant engineer at Samsung Electronics Co. Ltd., Gyeunggi-Do, South Korea. His interest is piezoelectric transformer power applications.